(10) T. M. Brown and B. L. Bush, *J. Less-Common Met.*, **25**, 397 (1971).
(11) "International Tables for X-Ray Crystallography", Vol. I, 2nd ed, Kynoch Press, Birmingham, England, 1965, p 135.
(12) L. V. Azaroff, *Acta Crystallogr.*, **8**, 701 (1955).
(13) A revised version of the Alcock analytical absorption program was used for this analysis.
(14) "International Tables for X-Ray Crystallography", Vol. IV, Kynoch Press, Birmingham, England, 1974, pp 99–101, 149–150.
(15) All calculations other than data reduction and absorption corrections were done using the "CRYSTALS" computing package: R. S. Rollett and J. R. Carruthers, personal communication.
(16) J. N. Smith and T. M. Brown, *Inorg. Nucl. Chem. Lett.*, **6**, 441 (1970).
(17) F. Bonati and R. Ugo, *J. Organomet. Chem.*, **10**, 257 (1967).
(18) E. L. Muetterties and L. J. Guggenberger, *J. Am. Chem. Soc.*, **96**, 1748 (1974).
(19) R. Hoffmann, B. F. Beier, E. L. Muetterties, and A. R. Rossi, *Inorg. Chem.*, **16**, 511 (1977).
(20) D. L. Kepert, *Inorg. Chem.*, **13**, 2754 (1974).
(21) The normalized bite is defined as the average S···S distance in the bite divided by the average Ta–S bond distance.

(22) M. Elder, *Inorg. Chem.*, **8**, 2103 (1969).
(23) J. J. Park, D. M. Collins, and J. L. Hoard, *J. Am. Chem. Soc.*, **92**, 3636 (1970).
(24) T. F. Brennan and I. Bernal, *Chem. Commun.*, 138 (1970); *Inorg. Chim. Acta*, **7**, 283 (1973).
(25) D. F. Lewis and R. C. Fay, *J. Am. Chem. Soc.*, **96**, 3834 (1974).
(26) R. B. Von Dreele, J. J. Stezowski, and R. C. Fay, *J. Am. Chem. Soc.*, **93**, 2887 (1971).
(27) R. B. Von Dreele, to be submitted for publication.
(28) J. C. Dewan, D. L. Kepert, C. L. Raston, D. Taylor, A. H. White, and E. N. Maslen, *J. Chem. Soc., Dalton Trans.*, 2082 (1973).
(29) J. C. Slater, *J. Chem. Phys.*, **41**, 3199 (1964).
(30) L. Pauling, "The Nature of the Chemical Bond", 3rd ed, Cornell University Press, Ithaca, N.Y., 1960, pp 224, 228, 274.
(31) D. van der Helm, A. E. Lessor, Jr., and L. L. Merritt, Jr., *Acta Crystallogr.*, **15**, 1227 (1962).
(32) R. Eisenberg, *Prog. Inorg. Chem.*, **12**, 295 (1970).
(33) D. Coucouvanis, *Prog. Inorg. Chem.*, **11**, 233 (1970).
(34) S. Esperas and S. Husebye, *Acta Chem. Scand.*, **26**, 3293 (1972).
(35) W. R. Busing and H. A. Levy, *Acta Crystallogr.*, **17**, 142 (1964).

Magnetic and Structural Characterization of Dibromo- and Dichlorobis(thiazole)copper(II)

WILLIAM E. ESTES, DIANE P. GAVEL, WILLIAM E. HATFIELD,* and DEREK J. HODGSON*

The temperature dependence of the magnetic susceptibility and the electron paramagnetic resonance spectra of the thiazole complexes dichloro- and dibromobis(thiazole)copper(II) are reported, along with a complete three-dimensional x-ray structure analysis of the dichloro complex based on counter data. The dichloro complex, $Cu(C_3H_3NS)_2Cl_2$, crystallizes in space group $P2_1/c$ of the monoclinic system with two independent formula units in a cell of dimensions $a = 7.332$ (6) Å, $b = 3.853$ (4) Å, $c = 17.493$ (17) Å, and $\beta = 93.70$ (1)°. The structure has been refined by full-matrix least-squares methods using 1172 independent data to a final value of the conventional R factor (on F) of 0.028. The structure, which consists of infinite chains of doubly chloride-bridged copper(II) ions, is reminiscent of those of the pyridine analogues, with a Cu–Cu separation of 3.853 (4) Å and bridging angle of 91.89 (2)°. The magnetic data and interchain exchange interactions are discussed in the light of the structural properties of the systems.

Introduction

Current interest in one-dimensional exchange-coupled magnetic systems has recently stimulated a considerable number of theoretical and experimental studies as well as several comprehensive reviews.[1-5] Most of the theoretical work has centered on completely *isolated* one-dimensional models, while the experimental work has reflected the longer range interactions which always occur in real crystals.

From the theoretical standpoint, most of the investigations have centered on the use of the various forms of the spin–spin Hamiltonian (1), where J is the exchange integral, S_x, S_y, and

$$H = -2J\Sigma_{i<j}[a\hat{S}_z{}^i \cdot \hat{S}_z{}^j + b(\hat{S}_x{}^i \cdot \hat{S}_x{}^j + \hat{S}_y{}^i \cdot \hat{S}_y{}^j)] \qquad (1)$$

S_z are the components of the total spin (S), the ratio a/b is an anisotropy parameter, and i and j label adjacent ions. For the case $a = 1$ and $b = 0$, the Ising model is obtained; and, in the special case for $S = 1/2$, an "exact" closed-form solution has been obtained for the magnetic and thermodynamic properties of a one-dimensional chain.[4-6] If the spins are restricted to lie in the xy plane, i.e., $a = 0$ and $b = 1$, then the X–Y or planar Heisenberg model is obtained; and Katsura[7] has obtained exact solutions for the $S = 1/2$ linear chain. Furthermore, when $a = b = 1$, the exchange interaction is isotropic and the Heisenberg model is obtained.[8-10]

Unfortunately, in the Heisenberg or isotropic limit, no closed-form solutions for magnetic or thermodynamic properties have yet been found; this being the case, almost all of *the theoretical analyses have used some approximations to estimate* the properties of linear chains.[9] Bonner and Fisher[8] studied the $S = 1/2$ antiferromagnetic Heisenberg chain and

performed computer calculations on finite rings and chains of isotropically interacting spins; they were able to estimate rather accurately the limiting behavior of the infinite linear system. Katsura and co-workers[11] have applied "linked-cluster" expansions via perturbation theory to estimate the various thermodynamic functions of interest. Finally, Baker, Rushebrooke, and co-workers[9,10] have employed a high-temperature series-expansion method to study the magnetic and thermal properties of linear Heisenberg systems. Generally, the results of Bonner and Fisher have been most widely accepted.[1]

Numerous experimental studies of linear-chain crystals have appeared in the literature.[1-3,5] The results of these experiments have been analyzed in terms of the available one-dimensional (1-D) models. Transitions to the long-range, three-dimensional ordered state have also been observed for several of these systems. Since it is known from the theorems of Mermin and Wagner[12] that pure one- and two-dimensional isotropic systems cannot sustain long-range order at finite temperatures, considerable interest has been focused on linear Heisenberg complexes with small but finite *interchain* exchange.[13,14]

Perhaps the most famous example of a nearly one-dimensional chain is provided by tetramethylammonium trichloromanganate(II) (TMMC), whose *intrachain* exchange is about 9 cm⁻¹ with longer range *interchain* interactions being about 4 orders of magnitude smaller.[16] For $S = 1/2$ complexes, copper tetraammine sulfate monohydrate (CTS) has been the most thoroughly studied,[17-21] but some recently reported electron paramagnetic resonance results have been interpreted in terms of a quadratic rather than linear model.[22] Finally, one of the best known examples of a $S = 1/2$ Heisenberg chain

Table I

Complex	J, cm^{-1}	Cu-X-Cu, deg	Cu-Cu, Å	Comments and Ref
Cu(tz)$_2$Cl$_2$	−3.69	92	3.85	1-D series
Cu(tz)$_2$Cl$_2$	−3.8	92	3.85	Bonner–Fisher
Cu(tz)$_2$Cl$_2$	−2.43	92	3.85	2-D series
Cu(4-Et(py))$_2$Cl$_2$	−6.7	92	4.00	28, 27a
Cu(4-vin(py))$_2$Cl$_2$	−9.1	90	4.04	28, 27b
Cu(py)$_2$Cl$_2$	−9.2	92	3.87	13, 15, 23, 25
Cu(3-Me(py))$_2$Cl$_2$	−8.9			28
Cu(3-Et(py))$_2$Cl$_2$	−11.9			28
Cu(tz)$_2$Br$_2$	−10.03			1-D series
Cu(tz)$_2$Br$_2$	−10.4			Bonner–Fisher
Cu(4-Me(py))$_2$Br$_2$	−14.8			28
Cu(4-Et(py))$_2$Br$_2$	−15.4			28
Cu(3-Me(py))$_2$Br$_2$	−15.5			28
Cu(py)$_2$Br$_2$	−18.9	93		15, 24
Cu(3-Et(py))$_2$Br$_2$	−22.3			28

is dichlorobis(pyridine)copper(II), in which the *intrachain* exchange is about 9 cm^{-1}, much larger than the observed *interchain* coupling.[13-15,23,24]

A relatively large number of transition-metal complexes of the general stoichiometry M^{II}L$_2$X$_2$ (where M is a divalent first-row metal ion, L is a heterocyclic nitrogen containing organic base, and X = Cl or Br) has been shown to contain,[24,27] or behave as if they contained, linear magnetic chains of doubly halogen-bridged metal ions.[13-15,23,28,29a,33,34] Typically, structural studies have shown that the ML$_2$X$_2$ systems contain doubly halogen-bridged metal ions with *intrachain* metal–metal distances of about 4 Å and M–X–M angles of about 90° (see Table I); these chains are usually packed in such a way that the *interchain* metal–metal distances are much longer (i.e., greater than 8 Å) than *intrachain* distances, and pseudo-one-dimensional chains are formed. Although *interchain* distances seem to imply quite weak interchain magnetic exchange, these effects have been observed; furthermore, it is believed that these weak *interchain* superexchange pathways involve M–X⋯N–M interactions. A thorough discussion of the properties of Cu(py)$_2$Cl$_2$ is available.[13,14]

With these facts in mind, the bis(thiazole)–dihalogen-metal(II) complexes reported by Underhill et al.[30] became of considerable interest. The structure of thiazole (C$_3$H$_3$NS) is depicted below. Since the electronic and infared spectra of

the thiazole complexes were similar to those of the known pyridine analogues, it was proposed that the compounds Cu(C$_3$H$_3$NS)$_2$X$_2$ were polymeric with double-halide bridges. Also, it might be expected that the sulfur atom of the heterocycle could provide an efficient *interchain* exchange pathway. In order to confirm the original postulates of Underhill et al. and to examine the possibility of enhanced interchain exchange we undertook low-temperature susceptibility and electron paramagnetic resonance studies of the complexes and a complete three-dimensional crystallographic analysis of the chloro complex. The results of these studies are reported here.

Experimental Procedure

Thiazole (C$_3$H$_3$NS, tz), obtained from Columbia Organic Chemicals, Columbia, S.C., was of *puriss* grade and was used without further purification. Reagent grade copper(II) chloride dihydrate and copper(II) bromide were obtained from J. T. Baker Chemical Co. and used directly.

Both complexes were prepared by a slight modification of the method described by Underhill et al.[30]

Dichlorobis(thiazole)copper(II), Cu(tz)$_2$Cl$_2$. To a warm solution of thiazole (0.51 g, 6 mmol) in ∼1 mL of absolute ethanol was added

0.5 g, (3 mmol) of CuCl$_2$·2H$_2$O in ∼8 mL of absolute ethanol. An immediate turquoise blue precipitate resulted; the mixture was stirred for 10 min, collected, washed with ether and benzene, and allowed to dry under suction. The product was recrystallized from dimethylformamide (DMF) by addition of an equal volume of methylene chloride followed by cooling in the freezer compartment of a refrigerator. Anal. Calcd for Cu(C$_6$H$_6$N$_2$S$_2$)Cl$_2$: C, 23.65; H, 1.98; Cl, 23.27. Found: C, 23.56; H, 2.08; Cl, 23.51.

Dibromobis(thiazole)copper(II), Cu(tz)$_2$Br$_2$. Cu(tz)$_2$Br$_2$ (hitherto not reported) was prepared as above. The dark green powder ($\bar{\nu}_{max}$ 14 285 cm^{-1}) was recrystallized as above to yield darker green hairlike needles. Anal. Calcd for Cu(C$_6$H$_6$N$_2$S$_2$)Br$_2$: C, 18.31; H, 1.55; Br, 40.6. Found: C, 18.31; H, 1.62; Br, 40.42.

Magnetic susceptibilities were obtained on a Princeton Applied Research Model 155 vibrating-sample magnetometer (VSM) operating at a field strength of 10 kG. Temperatures at the sample were measured with a calibrated GaAs diode by observing the voltage on a Dana Model 4700 4.5-place digital voltmeter; further details of the apparatus and temperature measurement have been given elsewhere.[31] Finely ground polycrystalline samples which were enclosed in Lucite sample holders typically weighed approximately 150 mg. The data were corrected for the diamagnetism of the Lucite holder and for the underlying diamagnetism of the constituent atoms using Pascal's constants.[32] A value of 60 × 10^{-6} cgsu was assumed for the temperature-independent paramagnetism (TIP).

Electron paramagnetic resonance (EPR) spectra were obtained at room temperature on a Varian E-3 spectrometer operating at approximately 9.5 GHz (X band). All spectra were recorded from very finely ground powders enclosed in commercially available quartz sample tubes. Several spectra were recorded at 77 K through the use of an insertion Dewar made by Varian. The magnetic field of the E-3 was calibrated by NMR techniques using a Magnion G-502 gaussmeter and a Hewlett-Packard 5340A frequency counter. The klystron frequency was observed directly with the frequency counter.

Determination of the Crystal Structure. Weissenberg and precession photographs indicated that the crystals belonged to the monoclinic system, the observed systematic absences of 0*k*0 for *k* odd and *h*0*l* for *l* odd being consistent only with the space group P2$_1$/c. The cell constants, determined by least-squares methods, are *a* = 7.332 (6) Å, *b* = 3.853 (4) Å, *c* = 17.493 (17) Å, and β = 93.70 (1)°; these observations were made at 21 °C with Mo Kα radiation with λ(Mo Kα) assumed as 0.7093 Å. A density of 2.03 g cm^{-3} obtained by flotation in carbon tetrachloride–bromoform mixtures is in acceptable agreement with the value of 2.05 g cm^{-3} calculated for two formula units per cell. Hence, in the centrosymmetric space group P2$_1$/c, the copper atom is constrained to lie on the inversion center.

Diffraction data were collected on a platelike crystal having faces (102), ($\bar{1}$0$\bar{2}$), (001), (00$\bar{1}$), (010), and (0$\bar{1}$0). The separations between opposite pairs of faces were as follows: (102) to ($\bar{1}$0$\bar{2}$), 0.0056 cm; (001) to (00$\bar{1}$), 0.014 cm; and (010) to (010), 0.061 cm. The crystal was mounted on a glass fiber parallel to the *b* axis, and data were collected on a Picker four-circle automatic diffractometer using Mo Kα radiation. The takeoff angle was 1.5°; at this angle the peak intensity of a typical strong reflection was approximately 95% of its maximum value. A total of 1761 reflections was examined by the θ–2θ scan technique at a scan rate of 1°/min. Allowance was made for the presence of both Kα$_1$ and Kα$_2$ radiations, the peaks being scanned from −1.0° in 2θ below the calculated Kα$_1$ peak position to +1.0° in 2θ above the calculated Kα$_2$ peak position. Stationary-counter, stationary-crystal background counts of 20 s were taken at each end of the scan.

A unique data set having 2θ < 60° was gathered. There were few reflections above background at values of 2θ > 60°. Throughout the data collection, the intensities of three standard reflections, measured every 100 reflections, remained essentially constant.

Data processing was carried out as described by Corfield et al.[36] After correction for background, the intensities were assigned standard deviations according to the formula[36]

$$\sigma(I) = [C + 0.25(t_s/t_b)^2(B_H + B_L) + (pI)^2]^{1/2}$$

with the value of *p* chosen to be 0.04. The values of *I* and σ(*I*) were corrected for Lorentz–polarization effects and for absorption factors. The absorption coefficient for the sample with Mo radiation is 31.25 cm^{-1}, and the transmission coefficients for the crystal data range from 0.56 to 0.87.[37] A total of 1761 reflections was collected, of which

Table II. Positional Parameters for [Cu(tz)$_2$Cl$_2$]

Atom	x	y	z
Cu	0.0	0.0	0.0
Cl	0.2023 (1)	0.3789 (2)	0.0646 (1)
S	−0.4279 (1)	0.0578 (2)	0.1697 (1)
N	−0.1567 (3)	0.0037 (5)	0.0888 (1)
C1	−0.3271 (3)	0.0998 (7)	0.0857 (1)
C2	−0.2286 (3)	−0.0916 (7)	0.2126 (1)
C3	−0.0990 (3)	−0.1038 (7)	0.1607 (1)
HC1	−0.383 (3)	0.167 (9)	0.042 (2)
HC2	−0.225 (4)	−0.149 (9)	0.256 (2)
HC3	0.019 (5)	−0.174 (10)	0.167 (2)

1172 were independent data with $I > 3\sigma(I)$; only these data were used in the final refinement of the structure.

Solution and Refinement of the Structure. All least-squares refinements were carried out on F minimizing the function $\sum w(|F_o| - |F_c|)^2$, with the weights w defined as $4F_o/\sigma^2(F_o^2)$. In all calculations of F_c the atomic scattering factors for all nonhydrogen atoms were taken from ref 38a and those for hydrogen taken from Stewart, Davidson, and Simpson.[39] The effects of the anomalous dispersion of Cu, S, and Cl were included in F_c, the values of $\Delta f'$ and $\Delta f''$ being taken from ref 38b. The unweighted and weighted residuals are defined as $R_1 = \sum ||F_o| - |F_c||/|F_o|$ and $R_2 = [\sum w(|F_o| - |F_c|)^2/\sum w(F_o)^2]^{1/2}$.

The location of the chlorine atom was determined from a three-dimensional Patterson function, the copper atom being assigned to the origin. Isotropic refinement of these positions gave $R_1 = 0.476$ and $R_2 = 0.540$. The positions of the remaining nonhydrogen atoms were determined from subsequent difference Fourier maps, and a least-squares refinement in which copper, chlorine, and sulfur were refined anisotropically while the nitrogen and carbon atoms were refined isotropically yielded values of R_1 and R_2 of 0.045 and 0.063, respectively. Anisotropic refinement of all of these atoms gave $R_1 = 0.034$ and $R_2 = 0.051$.

The three hydrogen atoms were located in a difference Fourier map; a least-squares refinement in which the nonhydrogen atoms were refined anisotropically and the hydrogen atoms were refined isotropically converged to values of R_1 and R_2 of 0.028 and 0.036, respectively, with the error in an observation of unit weight being 1.41.

Examination of the values of $|F_c|$ and $|F_o|$ suggested to us that no correction for secondary extinction was necessary, and none was applied. In the final cycle of least-squares refinement, there were 1172 observations and 73 variables, a reflection to variable ratio of 16:1. In this final cycle, no parameter underwent a shift of more than 0.13σ, which is taken as evidence of convergence. The value of R_2 shows no unusual dependence on $|F_o|$ or on sin θ, which suggests that our weighting scheme is adequate. A final difference Fourier showed two peaks of height 0.67 e Å^{-3} near the copper and chlorine atoms, which are presumably due to some small error in either our absorption correction or the anisotropic thermal model. No other peak higher than 0.58 e Å^{-3} was observed. The positional and thermal parameters derived from this final cycle, along with their standard deviations as estimated from the inverse matrix, are presented in Tables II and III. A compilation of observed and calculated structure amplitudes is available.[40]

Description of the Structure

The complex consists of square-planar Cu(tz)$_2$Cl$_2$ units which are linked by chloride bridges to form linear chains. The structure of each chain is, therefore, quite similar to that of
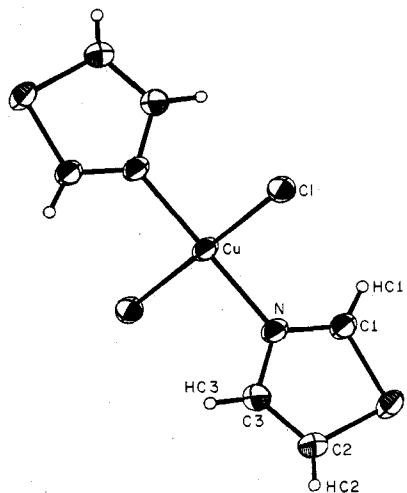

Figure 1. View of a single formula unit of Cu(tz)$_2$Cl$_2$. Hydrogen atoms are shown as open circles of arbitrary size. The view direction is parallel to the crystallographic b axis.

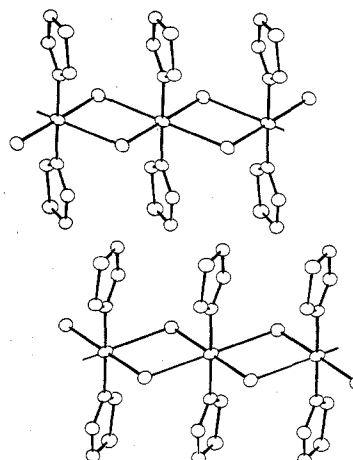**Figure 2.** View of the chain structure in Cu(tz)$_2$Cl$_2$. The view direction is parallel to the crystallographic a^* axis.

Cu(py)$_2$Cl$_2$.[24] A view of the square-planar array around a single copper ion is shown in Figure 1, and a view of the chain is given in Figure 2. The overall coordination around copper is, as can be seen in this figure, the commonly occurring (4 + 2) tetragonally elongated octahedral. The base plane is formed by the nitrogen atoms of two trans thiazole groups and by two chloride ions, the axial ligands being chloride ions which are in the base planes of the copper centers above and below. The base plane is strictly planar, there being a crystallographic inversion center at copper. The Cu–N and Cu–Cl (in plane) distances of 1.990 (2) and 2.322 (1) Å, respectively, are normal and comparable to values[24] of 2.004 (2) and 2.299 (2) Å in Cu(py)$_2$Cl. The out-of-plane Cu–Cl' distance of 2.998 (1) Å is slightly shorter than the value of 3.026 (2) Å in Cu(py)$_2$Cl$_2$

Table III. Thermal Parameters (U_{ij}) (Å^2) for [Cu(tz)$_2$Cl$_2$]

Atom	U_{11}	U_{22}	U_{23}	U_{12}	U_{13}	U_{23}
Cu	0.0246 (2)	0.0337 (2)	0.0205 (2)	−0.0064 (2)	0.0076 (1)	−0.0068 (2)
Cl	0.0274 (2)	0.0279 (3)	0.0264 (2)	−0.0022 (2)	0.0021 (2)	−0.0033 (2)
S	0.0287 (3)	0.0369 (3)	0.0300 (3)	0.0029 (2)	0.0118 (2)	0.0002 (2)
N	0.0244 (8)	0.0284 (10)	0.0212 (8)	−0.0017 (7)	0.0056 (6)	−0.0035 (7)
C1	0.0276 (10)	0.0306 (12)	0.0232 (10)	0.0002 (9)	0.0045 (8)	0.0007 (9)
C2	0.0332 (11)	0.0286 (12)	0.0215 (10)	−0.0012 (9)	0.0034 (9)	0.0029 (8)
C3	0.0267 (10)	0.0302 (12)	0.0266 (10)	0.0015 (9)	0.0021 (8)	−0.0000 (9)
HC1	$U = 0.017$ (8)					
HC2	$U = 0.013$ (7)					
HC3	$U = 0.023$ (8)					

[a] The form of the anisotropic thermal ellipsoid is exp$[-2\pi^2(U_{11}h^2a^{*2} + U_{22}k^2b^{*2} + U_{33}l^2c^{*2} + 2U_{12}hka^*b^* + 2U_{13}hla^*c^* + 2U_{23}klb^*c^*)]$.

Table IV. Distances (A) and Angles (deg) in Cu(tz)$_2$Cl$_2$

Distances

Cu–Cu′ [a]	3.853 (4)	S–C1	1.694 (2)
Cu–Cl	2.322 (1)	S–C2	1.700 (2)
Cu–Cl′	2.998 (1)	C2–C3	1.358 (3)
Cu–N	1.990 (2)	C1–HC1	0.877 (27)
N–C1	1.301 (3)	C2–HC2	0.794 (30)
N–C3	1.365 (3)	C3–HC3	0.906 (33)

Angles

Cl′–Cu–N	90.45 (6)	C1–S–C2	90.3 (1)
Cl–Cu–N	89.90 (6)	S–C2–C3	109.5 (2)
Cu–Cl–Cu′	91.89 (2)	N–C1–HC1	120.7 (18)
Cu–N–C1	124.8 (2)	S–C1–HC1	125.1 (17)
Cu–N–C3	123.8 (2)	S–C2–HC2	119.3 (22)
C1–N–C3	111.3 (2)	C3–C2–HC2	131.0 (22)
N–C1–S	113.1 (2)	N–C3–HC3	115.7 (19)
N–C3–C2	114.7 (2)	C2–C3–HC3	129.6 (19)

[a] A prime denotes a translation of the molecule along the *b* axis.

but is comfortably within the range of 2.698–3.37 Å reported for such distances in tetragonal-pyramidal dichloro-bridged copper(II) dimers.[41] The Cu–Cl–Cu′ bridging angle of 91.89 (2)° is again comparable to the value of 91.52 (5)° in Cu(py)$_2$Cl$_2$.

The bond lengths and angles in the molecule are listed in Table IV. The bond lengths in the thiazole moiety appear to be typical of those found in other conjugated ring systems. The thiazole ring is approximately planar, with no atom deviating from the best least-squares plane by more than 0.006 Å. The ring plane is inclined at an angle of 60° from the base plane of the copper octahedron.

It is noteworthy that the sulfur atom does not participate in coordination to the metal. The only possible interaction involving sulfur is an interchain S···S separation of 3.619 (1) Å; this value, which is slightly less than twice the reported[42] value (1.85 Å) of the van der Waals radius of sulfur, may indicate a weak interchain interaction in the crystals (vide infra).

While the geometry at any given copper atom in Cu(tz)$_2$Cl$_2$ is very similar to that in Cu(py)$_2$Cl$_2$, the arrangement of the chains in the crystal is quite different. In Cu(py)$_2$Cl$_2$, the "square planes" in each chain are parallel,[24] but this is not the case in the thiazole complex; in Cu(tz)$_2$Cl$_2$, the angle between the normals to the planes in adjacent chains is 77.89°. Consequently, to the extent that interchain interactions are significant (vide infra) there is an important structural distinction between the two complexes.

Results and Discussion

The compounds Cu(tz)$_2$Cl$_2$ and Cu(tz)$_2$Br$_2$ exhibited very broad, weak symmetrical bands centered at 14 400 and 14 300 cm^{-1}, respectively; furthermore, the shape and width of these d–d bands were noted to be very similar to those observed for Cu(py)$_2$Cl$_2$ (14 600 cm^{-1}) and Cu(py)$_2$Br$_2$ (14 600 cm^{-1})[43] except for a slight shift to lower energy. This shift seems reasonable since it is known that thiazole is a weaker base than pyridine.[30] In addition, there were no transitions in the region 16 000–17 000 cm^{-1} as have been observed[43] for the Cu(2-Me(py))$_2$X$_2$ compounds,[44] which are known to contain copper ions in a distorted square-based pyramidal array. Several intense higher energy bands were also observed for both complexes, these being centered at about 32 250 (strong) and 41 700 cm^{-1} for Cu(tz)$_2$Cl$_2$ and 23 250 (strong), 31 250 (strong), 32 000 (shoulder), and 41 700 cm^{-1} for Cu(tz)$_2$Br$_2$. These bands are either charge-transfer or intraligand transitions.[45] The observed electronic spectra are consistent with a distorted octahedral CuN$_2$X$_4$ chromophore as reported in extensive studies of the substituted-pyridine copper halide complexes.[43]
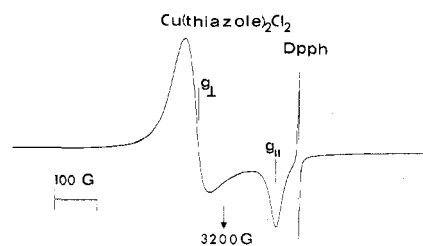

Figure 3. Room-temperature EPR spectrum (X band) of polycrystalline Cu(tz)$_2$Cl$_2$. The resonance fields show no temperature dependence down to 77 K.

Electron paramagnetic resonance (EPR) spectra were obtained on finely ground polycrystalline samples of both complexes. A single broad (~300 G) featureless line centered at $g \approx 2.11$ was observed for Cu(tz)$_2$Br$_2$; no appreciable temperature dependence was noted for this absorption down to ~77 K (the low-temperature limit of this investigation). Although virtually no quantitative information could be obtained from these spectra, it should be noted that qualitatively similar spectra have been observed in the bis(substituted-pyridine) complexes with copper bromide.[28] However, the EPR spectrum obtained for Cu(tz)$_2$Cl$_2$ (see Figure 3) is quite different from that normally seen for tetragonally distorted octahedral copper complexes. Indeed, an axial "reversed" spectrum was observed with $g_\perp$ (2.16) greater than $g_\parallel$ (2.04) and $\langle g \rangle$ = 2.11. Upon cooling the sample, the intensity of the highest field resonance increased slightly. The resonance fields remained constant within experimental error.

Since powder EPR spectra can only yield information about the values of the crystal **g** tensors,[47] additional analyses based on the molecular structure must be invoked to understand the observed "reversed" spectrum. One possibility is that the single-ion electronic ground state about the copper(II) ions is largely d$_{z^2}$.[46,47] If only discrete molecular units are considered, several stereochemistries have been shown to give rise to a species with a d$_{z^2}$ ground state:[47] (i) trigonal bypyramidal, (ii) tetragonally compressed octahedral, (iii) cis-distorted octahedral, and (iv) rhombically distorted octahedral. However, the x-ray structural results show that these stereochemistries do not obtain for Cu(tz)$_2$Cl$_2$. In this case, it is far more likely that the single-ion ground state is largely d$_{x^2-y^2}$, and the observed resonance is determined by inequivalent sites within the unit cell.[48,55–57] Since the two sites within the unit cell are magnetically inequivalent in the *ac* plane, the relative orientations of the tetragonally elongated octahedra will determine the observed crystal **g** tensors. Even though these molecular sites do not possess tetragonal site symmetry, this approximation allows for a much simpler relationship of the site **g** tensors to the observed powder **g** tensors. These expressions are given by (2), where $g'_\parallel$ and $g'_\perp$ are the observed

$$g'_\parallel{}^2 = g_\perp{}^2$$

$$g'_\perp{}^2 = g_\perp{}^2 \cos \delta^2 \alpha + g_\parallel{}^2 \sin^2 \alpha \qquad (2)$$

crystal *g* values, $g_\parallel$ and $g_\perp$ are the site *g* values for the tetragonally elongated octahedra about the copper(II) ions, and 2α is the angle between the tetragonal axes of the sites. If one assumes that *molecular* $g_\parallel$ is roughly normal to the plane of the four short bonds,[13,14] then the angle between the normals to these two sites is 77.89° for Cu(tz)$_2$Cl$_2$. Using this value of 2α and eq 2, the molecular *g* values are $g_\parallel$ = 2.23 and $g_\perp$ = 2.04. These values are in excellent agreement with those of the structurally similar Cu(py)$_2$Cl$_2$ complex.[13,14] In another rather similar system, β-Cu(NH$_3$)$_2$Cl$_2$ doped into the NH$_4$Cl host lattice, Tomlinson et al.[50] observed a "reversed" powder spectrum with $g'_\parallel$ = 2.006 and $g'_\perp$ = 2.175 and proposed that the geometry about copper was tetragonally compressed
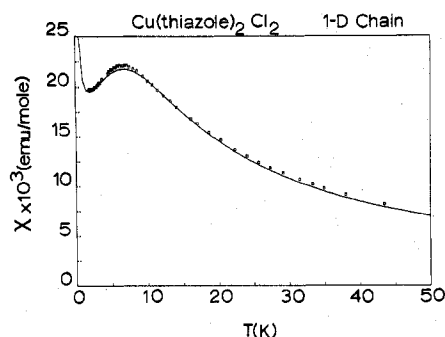
Figure 4. The temperature dependence of the magnetic susceptibility of $Cu(tz)_2Cl_2$. The observed data are shown as boxes, while the solid line represents the best fit to the Bonner–Fisher expression (see text) with $J = -3.81$ cm^{-1} and $g = 2.06$.
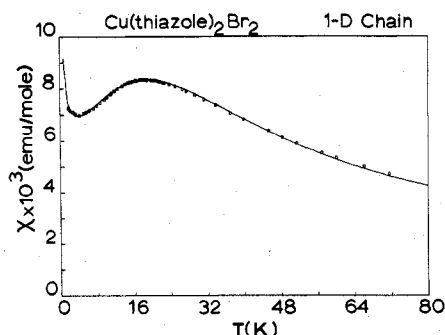

Figure 5. The temperature dependence of the magnetic susceptibility of $Cu(tz)_2Br_2$. The solid line represents the best fit to the Bonner–Fisher expression (see text) with $J = -10.4$ cm^{-1} and $g = 2.12$.

octahedral thus yielding a d_{z^2} ground state. However, it is also of interest to note that this cubic cell requires the molecular tetragonal axes to be oriented randomly, but any pair of axes are exactly 90° apart. Thus, such a system will always show a "reversed" powder spectrum irrespective of whether the sites are tetragonally elongated or compressed. This unusual circumstance arises because the 90° misalignment of the *molecular* parallel g values yields a unique perpendicular resonance (occurring at higher field) and a lower field, more intense resonance which is the average of the molecular parallel and perpendicular g values.

The experimental magnetic susceptibilities vs. absolute temperature for both complexes are plotted in Figures 4, 5, and 6. The data for the chloride complex are seen to exhibit a broad maximum at about 7 K, while the bromide analogue displays similar behavior at ca. 19 K. As can be seen from closer examination of the experimental data, the susceptibilities of both compounds appear to tend toward a nonzero value as the temperatures approach zero; this is just the behavior expected for an infinite linear chain since it is well-known that, in small clusters containing even multiples of $S = 1/2$, the susceptibility tends to zero as the temperature tends to zero (see ref 8). Also, inspection of the observed data [especially those of $Cu(tz)_2Br_2$] reveals a small Curie-like tail at the very lowest temperatures; phenomena similar to these have often been observed in similar systems[28,51] and have been attributed to the presence of small amounts of monomeric impurities (usually less than 1%) that become trapped in the material during synthetic procedures. Since these compounds are quite insoluble in all but strongly coordinating solvents (DMF), it was not possible to completely remove these impurities.

In the light of the observed crystal structure of $Cu(tz)_2Cl_2$ and the similarity of the observed electronic spectra of $Cu(tz)_2X_2$ with those of $Cu(py)_2X_2$, it is apparent that the magnetic data of the two systems should be comparable. As was noted in the Introduction, in the Ising limit (i.e., $b = 0$
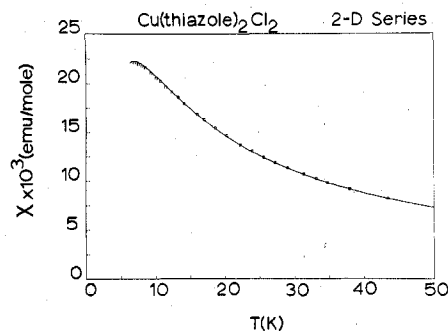

Figure 6. The high-temperature susceptibility, $kT/|J| \geq 1.6$, compared to the theoretical model of a two-dimensional Heisenberg layer (see text) with $J = -2.43$ cm^{-1} and $g = 2.11$.

in eq 1), Fisher[6] has obtained closed-form expressions for the susceptibility of a $S = 1/2$ linear-chain polymer. Although these equations are readily manipulated during fitting procedures, it has been generally accepted[52] that the totally anisotropic model is not appropriate for copper(II) ions. Furthermore, attempts to fit the data for the $Cu(tz)_2X_2$ complexes with this model resulted in unacceptable parameters and rather poor agreement between the observed and calculated susceptibilities.

de Jongh and Miedema[1] have suggested that the isotropic Heisenberg model (eq 1, $a = b = 1$) is probably more appropriate for systems with small **g** tensor anisotropy. Although there are no closed-form solutions known for the linear Heisenberg model, there are two approximations which can be used to estimate the exchange interaction from susceptibility data. Bonner and Fisher[8] have shown that the position of the maximum in the antiferromagnetic susceptibility can be estimated by the relationships $kT_{max}/|J| \approx 1.282$ and $|J|\chi_{max}/g^2\beta^2N \approx 0.0735$. Furthermore, Hall et al.[53] have recently been able to fit the Bonner–Fisher curve to the following rational function of $|J|/kT$:

$$\chi \approx \frac{Ng^2\beta^2}{kT} \frac{0.25 + 0.14995X + 0.30094X^2}{1.0 + 1.9862X + 0.68854X^2 + 6.0626X^3} \quad (3)$$

where

$$X = |J|/kT$$

The general form of eq 2 has been verified by comparing the susceptibilities thus calculated with those obtained from the high-temperature series expansion (HTS) of Baker et al.[10a]

$$\frac{\chi kT}{4Ng^2\beta^2} \approx [(1.0 + 5.97979916K + 16.902653K^2 +$$

$$29.376885K^3 + 29.832959K^4 + 14.036918K)^5/(1.0 +$$

$$2.7989916K + 7.008678K^2 + 8.0538644K^3 +$$

$$4.5743114K^4)]^{2/3} \quad (4)$$

where

$$K = J/2kT$$

The above series has been normalized to the Curie law for $J = 0$ (i.e., $\chi = Ng^2\beta^2S(S + 1)/3kT$ since Baker et al.[10a] did not include the factor of 4 (i.e., $S(S + 1)/3$) in the denominator. In the temperature range of $kT/|J| > 1.25$, agreement between susceptibilities calculated by eq 2 and 3 was excellent, with all disparities being less than 1%.

In view of the probable presence of impurities at temperatures low compared to T_{max}, it was reasoned that fitting the data to the result of Baker et al.[10] would be the most acceptable initial attempt. This is reasonable because at χ_{max} and above the presence of the impurity can be neglected. In order to fit the data to eq 3, $|J|$ was estimated from the corresponding

temperature using Bonner and Fisher's relations and the experimental data below $kT/|J| = 1.25$ were omitted (i.e., those below 7 and 18 K for the chloride and bromide, respectively). The best fits of the data to eq 3 were $\langle g \rangle = 2.06$, $J = -3.7$ cm^{-1} and $\langle g \rangle = 2.11$, $J = -10.3$ cm^{-1} for the chloride and bromide complexes, respectively (see Table I).

To gain more information about the low-temperature behavior of the data $(kT/|J| \leq 1.25)$, we have compared it to the results of Bonner and Fisher (eq 3). In making this comparison, the presence of monomeric impurities was allowed for by assuming that $\chi_{obsd} = \chi_{chain} + \chi_{impurity}$. Furthermore, by assuming that the impurity obeys the Curie law, the following expression for the total susceptibility results:[54]

$$\chi_{obsd} = \left\{ \frac{P[Ng^2\beta^2 S(S+1)]}{3kT} + (100 - P)\chi_{chain} \right\}/100 \quad (5)$$

where $S = \frac{1}{2}$, $P = \%$ impurity, and $g = $ observed average g value from the EPR spectra. For the fit using the approximation of the Bonner–Fisher curve, J and P were allowed to vary in the fitting routine. The best fits obtained in this manner were $J = -10.3$ cm^{-1}, $P = 0.65\%$ and $J = -3.97$ cm^{-1}, $P = 1.46\%$ for the bromide and chloride complexes, respectively. In order to check the validity of the impurity correction, the next fits were performed by allowing g, J, and P to vary simultaneously; this resulted in $J = -10.4$ cm^{-1}, $g = 2.12$, and $P = 0.66\%$ for $Cu(tz)_2Br_2$ and $J = -3.81$ cm^{-1}, $g = 2.06$, and $P = 1.35\%$ for $Cu(tz)_2Cl_2$. These fits are shown in Figures 4 and 5. Although both of the linear models appear to provide an excellent description of the susceptibility data of $Cu(tz)_2Br_2$, the validity of this approach for $Cu(tz)_2Cl_2$ may be in question since there are large differences in the exchange constants between $Cu(tz)_2X_2$ and $Cu(py)_2X_2$ while the structural details for the two compounds are very similar. Since the magnitude of the maximum in the antiferromagnetic susceptibility is determined by the g value for a given J, a discrepancy in this portion of the fit may imply that the model chosen is inappropriate. Thus, as the dimensionality of the magnetic interaction increases, the position of the maximum in reduced coordinates becomes lower and the χ vs. T curve becomes broader.[1]

The similarity of the structures of $Cu(tz)_2Cl_2$ and $Cu(py)_2Cl_2$ and the relatively large differences in the exchange constants for the one-dimensional analyses suggest that the magnetic interactions in the thiazole complexes are of higher dimensionality. Hence, the magnetic susceptibility data were compared to the Bonner–Fisher theory assuming a first-order molecular field correction to account for interchain interactions,[59] eq 6, where χ_{B-F} is the susceptibility of an isolated

$$\chi = \frac{\chi_{B-F}}{1 - \frac{2zJ'\chi_{B-F}}{Ng^2\beta^2}} \quad (6)$$

Heisenberg chain, J' is the interchain exchange, and z is the number of nearest neighbors. In the calculations the g value was fixed to that observed by EPR and J and zJ' were allowed to vary freely. This approach led to best-fit values of $J = -3.31$ cm^{-1}, $J'(Z = 4) = 1.55$ cm^{-1}, and $\langle g \rangle = 2.11$ for $Cu(tz)_2Cl_2$ while the data for the bromo compound yielded $J = -10.48$ cm^{-1}, $zJ' = +1.14$ cm^{-1}, and $\langle g \rangle = 2.11$. Although this modified one-dimensional model makes a crude approximation to the interchain interactions present, it fails to describe the susceptibility of $Cu(tz)_2Cl_2$ near the maximum since deviations of about 5% between the observed and calculated susceptibilities occur. Furthermore, the sum of the squares of the deviations of a point from the calculated curve, $SD = \sum((\chi_{obsd} - \chi_{calcd})/\chi_{obsd})^2$, is 1.81×10^{-2}. The fit of the data for the bromo compound is hardly affected by the interchain term. The failure of the molecular-field approach for $Cu(tz)_2Cl_2$ was

not totally unexpected since molecular-field theory is a very poor model for low-dimensional systems.[1]

To investigate the possibility that the magnetic interactions in $Cu(tz)_2Cl_2$ were of higher dimensionality, the data were fitted to the high-temperature series expansion for the two dimensional Heisenberg antiferromagnetic layer[10b,58]

$$\chi_{2D} = \frac{Ng^2\beta^2}{4kT}[1 - 2(J/kT) + 2(J/kT)^2 + \ldots] \quad (7)$$

Although an argument based soley on the metal–metal distances and strongly bonded ligands would imply that a 2-D planar model with four nearest neighbors should not be appropriate for this compound, inspection of the unit cell reveals that a superexchange pathway via the short sulfur–sulfur contacts does exist in the ac plane. Furthermore, an excellent fit over the range $kT/|J| \geq 1.6$ can be obtained using eq 7. This leads to a best-fit value of $J = -2.43$ cm^{-1} (see Figure 6) when only J is varied and the experimentally determined g value from EPR, $g = 2.11$, is used. The criterion of the fit, $((\chi_{obsd} - \chi_{calcd})/\chi_{obsd})^2 = 2.28 \times 10^{-4}$, is 3 orders of magnitude better than that found for the molecular-field model fit. Attempts to fit the data for $Cu(tz)_2Br_2$ to the 2-D series were unsuccessful and led to deviations as high as 8% from the calculated curve near the maximum.

The magnetic and structural properties of the $Cu(tz)_2X_2$ systems are compared in Table I with those previously observed for their substituted-pyridine analogues. The magnitude of the exchange, $|J|$, for both of the thiazole compounds is considerably smaller than those reported for the $Cu(py)_2X_2$ compounds if one takes the values determined from the linear-chain models. This is surprising in view of the similarity between the structures of $Cu(tz)_2Cl_2$ and $Cu(py)_2Cl_2$; in the former, the $Cu-Cl-Cu'$ bridge angle and $Cu-Cl$ out-of-plane distances are 91.89 (2)° and 2.998 (1) Å, respectively, while the analogous values in $Cu(py)_2Cl_2$ are 91.52 (5)° and 3.026 (2) Å. The observation may be the result of a much larger *interchain* exchange for the thiazole complexes since the 2-D model can be used to approximate the data of $Cu(tz)_2Cl_2$. Presumably, the additional superexchange pathway via sulfur–sulfur contacts between chains plays a very important role in this dimensionality increase.

References and Notes

(1) L. J. de Jongh and A. R. Miedema, *Adv. Phys.*, **23**, 1 (1974).
(2) C. Domb and A. R. Miedema, *Prog. Low Temp. Phys.*, **4**, Chapter 4 (1966).
(3) J. Ackerman, G. Cole, and S. L. Holt, *Inorg. Chim. Acta*, **8**, 323 (1972).
(4) E. Lieb and D. C. Mattis, "Mathematical Physics in One Dimension", Academic Press, New York, N.Y., 1966, Chapter 6.
(5) D. Hone and P. M. Richards, *Annu. Rev. Mater. Sci.*, **4**, 337 (1974).
(6) M. E. Fisher, *J. Math. Phys. (N.Y.)*, **4**, 124 (1963), and references therein.
(7) S. Katsura, *Phys. Rev.*, **127**, 1508 (1962); **129**, 2835 (1963).
(8) J. C. Bonner and M. E. Fisher, *Phys. Rev. [Sect.] A*, **135**, A640 (1964), and references therein.
(9) G. A. Baker, G. S. Rushbrooke, and P. W. Wood, *Phase Transitions Crit. Phenom.*, **3**, 246 (1974).
(10) (a) G. A. Baker, G. S. Rushbrooke, and H. Gilbert, *Phys. Rev. [Sect.] A*, **135**, A1272 (1964); (b) G. S. Rushbrooke and P. W. Wood, *Mol. Phys.*, **1**, 257 (1958); (c) G. S. Rushbrooke and P. W. Wood, *Proc. Phys. Soc., London, Sect. A*, **68**, 1161 (1955).
(11) S. Inawashiro and S. Katsura, *Phys. Rev. [Sect.] A*, **140**, A892 (1965), and references therein.
(12) N. D. Mermin and H. Wagner, *Phys. Rev. Lett.*, **17**, 1133 (1967).
(13) W. Duffy, J. Venneman, D. Strandberg, and P. M. Richards, *Phys. Rev. B*, **9**, 2220 (1974).

(14) R. Hughes, B. Morosin, P. M. Richards, and W. Duffy, *Phys. Rev. B*, **11**, 1795 (1975), and references therein.
(15) D. Y. Jeter and W. E. Hatfield, *J. Inorg. Nucl. Chem.*, **34**, 3055 (1972).
(16) (a) L. R. Walker, R. Dietz, K. Andres, and S. Darack, *Solid State Commun.*, **11**, 593 (1972); (b) C. Bupas and J.-P. Renard, *Phys. Lett. A*, **43**, 119 (1973).
(17) J. J. Fritz and H. L. Pinch, *J. Am. Chem. Soc.*, **79**, 3644 (1957).
(18) T. Haseda and A. R. Miedema, *Physica (Utrecht)*, **27**, 1102 (1961).
(19) T. Watanabe and T. Haseda, *J. Chem. Phys.*, **29**, 1429 (1958).
(20) F. Mazzi, *Acta Crystallogr.*, **8**, 137 (1955).
(21) R. B. Griffiths, *Phys. Rev. [Sect.] A*, **135**, 659 (1964).
(22) M. Date, M. Motokawa, H. Hori, S. Kuroda, and K. Matsui, *J. Phys. Soc. Jpn.*, **39**, 257 (1975).
(23) K. Takeda, S. Matsukawa, and T. Hageda, *J. Phys. Soc. Jpn.*, **30**, 1330 (1971).
(24) B. Morosin, *Acta Crystallogr., Sect. B*, **31**, 632 (1975).
(25) S. Gorter, A. van Ingen Schenan, and G. Vershoor, *Acta Crystallogr., Sect. B*, **30**, 1867 (1974).
(26) P. M. Richards, R. Quinn, and B. Morosin, *J. Chem. Phys.*, **59**, 4474 (1973).
(27) (a) M. Laing and E. Horsfield, *Chem. Commun.*, 735 (1968); (b) *ibid.*, 902 (1969); (c) M. Laing and G. Garr, *J. Chem. Soc. A*, 1141 (1971).
(28) V. H. Crawford and W. E. Hatfield, *Inorg. Chem.*, **16**, 1336 (1977).
(29) (a) H. T. Witteven, Ph.D. Thesis, University of Leiden, 1973; (b) H. T. Witteven and J. Reedijk, *Solid State Commun.*, **10**, 151 (1974).
(30) W. Eilbeck, T. Holmes, and A. E. Underhill, *J. Chem. Soc. A*, 757 (1967).
(31) D. B. Losee and W. E. Hatfield, *Phys. Rev. B*, **10**, 212 (1974).
(32) P. W. Selwood, "Magneto Chemistry", Interscience, New York, N.Y., 1956.
(33) (a) F. Klaaijsen, H. Blote, and Z. Dokoupil, *Solid State Commun.*, **14**, 607 (1974); (b) S. Foner, R. Frankel, W. Reiff, B. Little, and G. Long, *ibid.*, **14**, 16 (1975); (c) H. T. Witteven, W. Ristten, and J. Reedijk, *J. Inorg. Nucl. Chem.*, **37**, 113 (1975).
(34) H. T. Witteven, B. Nieiuvenhuijse, and J. Reedijk, *J. Inorg. Nucl. Chem.*, **36**, 1535 (1975).
(35) J. E. Wertz and J. R. Bolton, "Electron Spin Resonance: Elementary Theory and Practical Applications", McGraw-Hill, New York, N.Y., 1972, p 465.
(36) P. W. R. Corfield, R. J. Doedens, and J. A. Ibers, *Inorg. Chem.*, **6**, 197 (1967).
(37) For a description of the programs used in this analysis, see D. L. Lewis and D. J. Hodgson, *Inorg. Chem.*, **13**, 143 (1974).
(38) "International Tables for X-Ray Crystallography", Vol. IV, Kynoch Press, Birmingham, England: (a) Table 2.2A; (b) Table 2.1 C.
(39) R. F. Stewart, E. R. Davidson, and W. T. Simpson, *J. Chem. Phys.*, **42**, 3175 (1965).
(40) Supplementary material.
(41) D. W. Phelps, W. H. Goodman, and D. J. Hodgson, *Inorg. Chem.*, **15**, 2266 (1976), and references therein.
(42) L. Pauling, "The Nature of the Chemical Bond", 3rd ed, Cornell University Press, Ithaca, N.Y., 1960.
(43) W. Ludwig and F. Gasser, *Helv. Chim. Acta*, **52**, 107 (1969).
(44) P. Singh, D. Y. Jeter, W. E. Hatfield, and D. J. Hodgson, *Inorg. Chem.*, **11**, 1657 (1972).
(45) B. Ellis and P. Griffiths, *Spectrochim. Acta*, **21**, 1881 (1965).
(46) K. T. McGregor and W. E. Hatfield, *J. Chem. Soc., Dalton Trans.*, 2448 (1974).
(47) B. J. Hathaway and D. E. Billing, *Coord. Chem. Rev.*, **5**, 143 (1970).
(48) K. T. McGregor and Z. G. Soos, *Inorg. Chem.*, **15**, 2159 (1976).
(49) R. Hegele and D. Babel, *Z. Anorg. Allg. Chem.*, **409**, 11 (1974).
(50) A. Tomlinson and B. J. Hathaway, *J. Chem. Soc. A*, 2578 (1968), and references therein.
(51) R. P. Eckberg and W. E. Hatfield, *Inorg. Chem.*, **14**, 1205 (1975).
(52) R. W. Jotham, *J. Chem. Soc., Chem. Commun.*, 178 (1973).
(53) J. W. Hall, W. E. Estes, and W. E. Hatfield, to be submitted for publication.
(54) A. P. Ginsberg, *Inorg. Chim. Acta, Rev.*, **5**, 45 (1971).
(55) J. E. Wertz and J. R. Bolton, "Electron Spin Resonance: Elementary Theory and Practical Applications", McGraw-Hill, New York, N.Y., 1972, Chapter 7, p 131 ff.
(56) J. A. Ibers and J. D. Swalen, *Phys. Rev.*, **127**, 1914 (1962).
(57) J. H. P. Colpa, *Physica (Utrecht)*, **57**, 347 (1972).
(58) C. A. Baker, H. E. Gilbert, J. Eve, and G. S. Rushbrooke, *Phys. Lett. A*, **25**, 3 (1967).
(59) J. N. McElerney, S. Merchant, and R. L. Carlin, *Inorg. Chem.*, **12**, 906 (1973).

Syntheses and Crystal Structures at −35 °C of Bis(η³-2-allyl)-1,2-ethanobis(tricarbonylcobalt) and Bis(η³-2-allyl)-1,3-propanonobis((trimethyl phosphite)dicarbonylcobalt)

KEVIN CANN, PAUL E. RILEY, RAYMOND E. DAVIS,* and ROWLAND PETTIT*

The two η³-allyl complexes {(CO)₃Co[(CH₂)₂CCH₂]}₂ and {(CO)₃Co[(CH₂)₂CCH₂]}₂CO have been prepared by reaction of (chloromethyl)allyl chloride and NaCo(CO)₄ in refluxing THF. Both species are formed during this reaction and may be converted to the trimethyl phosphite derivatives by replacement of one CO ligand per Co atom. The structures of {(CO)₃Co[(CH₂)₂CCH₂]}₂ and {[(CH₃O)₃P](CO)₂Co[(CH₂)₂CCH₂]}₂CO have been determined by single-crystal x-ray diffraction techniques with three-dimensional data gathered at −35 °C by counter methods. Bulky yellow crystals of {(CO)₃Co[(CH₂)₂CCH₂]}₂ form in monoclinic space group $C2/m$, with unit cell constants (at −35 °C) $a = 11.570$ (3) Å, $b = 10.910$ (2) Å, $c = 6.568$ (1) Å, and $\beta = 99.95$ (1)°. The calculated density of 1.583 g cm⁻³, assuming two molecules of {(CO)₃Co[(CH₂)₂CCH₂]}₂ per unit cell, agrees with the measured value of 1.57 g cm⁻³. {[(CH₃O)₃P](CO)₂Co[(CH₂)₂CCH₂]}₂CO crystallizes as thin yellow prisms in orthorhombic space group $P2_12_12$, with unit cell constants (at −35 °C) $a = 19.688$ (4), $b = 20.843$ (10), and $c = 6.532$ (2) Å. The calculated density of 1.528 g cm⁻³ for four molecules of phosphite complex per unit cell agrees with the measured value of 1.50 g cm⁻³. Full-matrix least-squares refinements of the structures have converged with R indices (on $|F|$) of 0.021 and 0.062 for the {(CO)₃Co[(CH₂)₂CCH₂]}₂ and {[(CH₃O)₃P](CO)₂Co[(CH₂)₂CCH₂]}₂CO complexes, respectively, using the 1168 and 2134 symmetry-independent reflections with $I_0 > 2.0\sigma(I_0)$. Molecules of {(CO)₃Co[(CH₂)₂CCH₂]}₂ possess rigorous C_{2h} symmetry and display the significant differences in Co–C(carbonyl) distances which have previously been attributed to the nature of the Co–η³-allyl interaction. Although molecules of {[(CH₃O)₃P](CO)₂Co[(CH₂)₂CCH₂]}₂CO have no rigorous crystallographic symmetry, they do exhibit approximate-C_2 symmetry. In addition to the Co–C(carbonyl) bond asymmetry noted in {(CO)₃Co[(CH₂)₂CCH₂]}₂, the substitution of P(OCH₃)₃ for CO has produced differences in the Co–C(allyl, terminal) bond lengths of {[(CH₃O)₃P](CO)₂Co[(CH₂)₂CCH₂]}₂CO.

Introduction

In 1960, Heck and Breslow reported the synthesis of the π-allylcobalt complex (η³-C₃H₅)Co(CO)₃, formed from the reaction of NaCo(CO)₄ and allyl bromide in ether at 25 °C.[1] To date, this remains the best method for the preparation of complexes of this kind. We have employed a similar procedure in our attempts to synthesize a precursor of a cobalt–trimethylenemethane complex; viz., NaCo(CO)₄ (1) and

(chloromethyl)allyl chloride (2) were refluxed in dry THF for 20 min. However, the products which were obtained were neither the mono-π-allylcobalt tricarbonyl of Heck and Breslow nor a desired precursor of a cobalt–trimethylenemethane complex but were, as subsequently determined, the two unexpected compounds 3 and 4.

The molecular structures of unknown compounds 3 and 4 were established by crystal structure analysis: 3 directly by